SUPPORTING INFORMATION

"An In Vivo Model of Ischemic Spinal Cord Injury in Awake Rats Identifies Early Mixed Macrophage Polarization and Impaired Inflammatory Resolution"

[1]Tagore G. de Morais[¶],[1]Caio Perret[¶], [2]Karsten Gronert, [3]Fred A. Lado, [1,4,5]Renato Rozental[*].

SI ILLUSTRATIONS

- 4 SUPPLEMENTARY FIGURES

SUPPORTING INFORMATION
de Morais et al. – Nature Spinal Cord

SI Materials and Methods

Ethics statement. All experimental procedures involving animals and human participants were conducted in accordance with the principles of the Declaration of Helsinki, where applicable, and the National Institutes of Health (NIH) Guide for the Care and Use of Laboratory Animals. The study was reviewed and approved by the respective Institutional Review Boards and Institutional Animal Care and Use Committees (IACUCs). Studies were approved by the Ethics Committees of the Federal University of Rio de Janeiro, Brazil (CAAE 37520820.4.3001.5259) and Hospital Municipal Miguel Couto, Rio de Janeiro, Brazil (CAAE 96263418.0.0000.5279). Animal experiments were approved by the Animal Ethics Committee of the Federal University of Rio de Janeiro (CEUA-UFRJ DAHEICB protocol 053), the Institutional Animal Care and Use Committee of New York Medical College, Valhalla, NY, USA (IACUC protocol 69-12-0609.1), and the Institutional Animal Care and Use Committee of Albert Einstein College of Medicine, Bronx, NY, USA (IACUC protocol 20030906).

Tissue collection, RNA extraction, microarray processing, and transcriptomic analysis. At 24 h after the onset of paralysis, nine independent biological samples were collected for transcriptomic analysis, comprising three uninjured control animals, three MES-stimulated animals that did not develop paralysis, and three MES-stimulated animals that developed persistent paralysis. The MES-stimulated groups were time-matched. Animals were deeply anesthetized and euthanized, and the thoracic SC segments spanning T8–T12, encompassing the T10 lesion epicenter, were rapidly dissected under RNase-free conditions. Tissue collection was completed within 3–5 min of euthanasia to minimize RNA degradation. Each specimen was immediately transferred to a sterile RNase-free cryovial, snap-frozen in liquid nitrogen, and stored at −80 °C. Samples were maintained continuously at −80 °C and transported on dry ice to Genome Explorations (Memphis, TN, USA) without freeze–thaw cycles.

Total RNA was extracted by Genome Explorations using standardized procedures optimized for neural tissue. RNA concentration and purity were assessed spectrophotometrically by measuring A260/A280 and A260/A230 ratios. RNA integrity was evaluated using microfluidic capillary electrophoresis with an Agilent 2100 Bioanalyzer (Agilent Technologies, Santa Clara, CA, USA). Samples with an RNA Integrity Number (RIN) ≥8.0 were considered suitable for downstream microarray analysis. Representative RNA quality-control profiles are shown in **Supplementary Fig. 3.**

Affymetrix microarray processing. High-quality RNA samples were processed for genome-wide expression profiling using Affymetrix Rat Genome 230 2.0 arrays according to the manufacturer's recommended procedures. Briefly, RNA was reverse-transcribed and amplified, and the resulting labeled complementary RNA was hybridized to the arrays. Following hybridization, arrays were washed,

stained, and scanned using the manufacturer's recommended instrumentation. Raw fluorescence intensity data were exported as CEL files for downstream computational analysis.

Microarray data preprocessing and normalization. CEL files were imported into R using the Bioconductor affy package. Because the Affymetrix Rat Genome 230 2.0 platform contains paired perfect-match (PM) and mismatch (MM) probes, the Microarray Suite 5.0 (MAS 5.0; Affymetrix) algorithm was used for probe-level background correction and probe-set summarization. MAS 5.0 processing also generated detection calls (Present, Marginal, or Absent), which were used to assess the repertoire of detectably expressed transcripts. Processed expression values were $\log_2$-transformed prior to downstream statistical analysis. Probe-set annotations were assigned using the rat2302.db Bioconductor annotation package.

Differential gene-expression analysis. Differential expressions were assessed using the limma package in R. Comparisons were performed among the three experimental groups, with particular emphasis on the contrasts between paralyzed animals and uninjured controls and between paralyzed and MES-stimulated non-paralyzed animals. Linear models were fitted to the normalized expression data, and empirical Bayes moderation was applied to the estimated variances. Multiple-testing correction was performed using the Benjamini–Hochberg procedure.

Genes were considered differentially expressed when they met both criteria of an adjusted P value <0.05 and an absolute $\log_2$ fold-change $\geq$ I1I. Differentially expressed genes were subsequently used for cellular-signature and pathway analyses described in the main text.

Biological pathway and gene-expression analysis. To characterize the biological processes associated with the transcriptional response to ischemic SCI, DEGs identified at 24 h were subjected to functional annotation and pathway-enrichment analyses. GO analysis was used to identify enriched biological processes, molecular functions, and cellular components, whereas KEGG and Reactome analyses were used to identify enriched signaling, metabolic, and cellular pathways. Analyses were performed using the Enrichr platform together with complementary gene-set enrichment approaches, and statistical significance was assessed using appropriate multiple-testing correction.

In addition to database-driven enrichment, pathway-level findings were examined within a literature-guided biological framework focused on processes known to contribute to the acute response to ischemic SCI. These included inflammatory signaling and innate immune activation, monocyte/macrophage recruitment and differentiation, astrocytic and microglial responses, lipid and fatty-acid metabolism, neuronal and axonal responses, and extracellular-matrix remodeling. These categories were used to facilitate biological interpretation of the enriched pathways rather than as independent statistical classifications.

Reactome analysis of highly upregulated transcripts. The 50 most strongly upregulated genes were examined individually and mapped to Reactome pathways to identify biological processes disproportionately represented among the most prominent transcriptional changes. Particular attention was given to immune-related pathways and genes associated with macrophage phenotypes, including Arg1, as well as pathways involved in circulating monocyte differentiation and resolution-associated programs linked to docosahexaenoic acid (DHA) metabolism.

Finally, pathway-level results were integrated with individual-gene expression patterns and with the biochemical, histological, and inflammatory findings obtained at the same 24-h time point. This integrative approach enabled interpretation of the transcriptomic response at both the individual-gene and biological-pathway levels, reducing reliance on isolated transcript changes and providing a framework for linking molecular alterations to the cellular and tissue responses observed after ischemic SCI.

Data deposition. The complete microarray dataset, including the raw CEL files and processed expression data, was deposited in the NCBI Gene Expression Omnibus (GEO) database in accordance with MIAME recommendations. The GEO accession number is provided in the Data Availability statement and will be included in the manuscript upon assignment.

SearchLight multiplex cytokine and chemokine assay. SC tissue samples were collected separately from the T8, T10, and T12 levels from three experimental groups: uninjured controls, MES-stimulated animals without paralysis, and MES-stimulated animals with persistent paralysis (n = 3 animals per group). Tissue homogenates were analyzed using the SearchLight® Multiplex Protein Array platform (Pierce Biotechnology, Inc., Woburn, MA, USA). The assay uses a multiplexed sandwich ELISA format in which analyte-specific capture antibodies are arrayed within individual wells. Following incubation with tissue homogenates, bound proteins were detected using biotinylated detection antibodies and streptavidin–horseradish peroxidase, followed by chemiluminescent detection using the SearchLight imaging system. Concentrations were determined from analyte-specific standard curves. The panel comprised Fractalkine (CX3CL1), GRO/KC (CXCL1), MCP-1 (CCL2), MIP-2 (CXCL2), RANTES (CCL5), IL-1β, IL-4, IL-6, and TNF-α. Each sample was analyzed in duplicate; the mean of the duplicate measurements was calculated and corrected for the corresponding sample dilution. Final concentrations were expressed as pg/mL. Statistical analysis were performed using ANOVA on Jamovi Software (2.6 version) following concentrations log10 transformation.

X-ray and magnetic resonance imaging. Spinal radiographs (n=5) were obtained on day 5 after paralysis at Jacobi Medical Center, Albert Einstein College of Medicine, Bronx, NY, using a Siemens Medical Systems conventional radiography system and standard clinical radiographic techniques. MRI was performed at the Gruss Magnetic Resonance Research Center (MRRC), Albert Einstein College of Medicine, Bronx, NY, using a 9.4-T Varian animal MRI/MRS system with a 21-cm bore**.** The system was designed for high-field small-animal anatomical imaging and spectroscopy and included dedicated rodent

radiofrequency coils and high-performance gradient/shim hardware. T2-weighted multislice spin-echo images were acquired from the brain and SC with repetition time (TR) = 1.5 s, echo time (TE) = 40 ms, and 1-mm slice thickness**.** Images were obtained on day 5 after the onset of MES-induced paralysis for anatomical characterization of the lesion (Felder *et al.* 2017). The use of this high-field platform for experimental rat MRI/MRS at Einstein has been previously reported (Miyasaka et al., 2006; Gomes et al., 2007).

SI REFERENCES

Felder J, Celik AA, Choi CH, Schwan S, Shah NJ. 9.4 T small animal MRI using clinical components for direct translational studies**.** *J Transl Med*. **15 (1)**, 264 (2017)

Gomes WA, Lado FA, de Lanerolle NC, Takahashi K, Pan C, Hetherington HP. Spectroscopic imaging of the pilocarpine model of human epilepsy suggests that early NAA reduction predicts epilepsy. *Magn Reson Med***. 58** (2), 230–235 (2007).

Miyasaka N, Takahashi K, Hetherington HP. Fully automated shim mapping method for spectroscopic imaging of the mouse brain at 9.4 T. *Magn Reson Med***. 55**,198–202 (2006).

Pfaffl MW. A new mathematical model for relative quantification in real-time RT-PCR. Nucleic Acids Res. **29(9):**e45 (2001).

The jamovi project. jamovi (**Version 2.7**) https://www.jamovi.org (2026).

SUPPLEMENTARY FIGURES

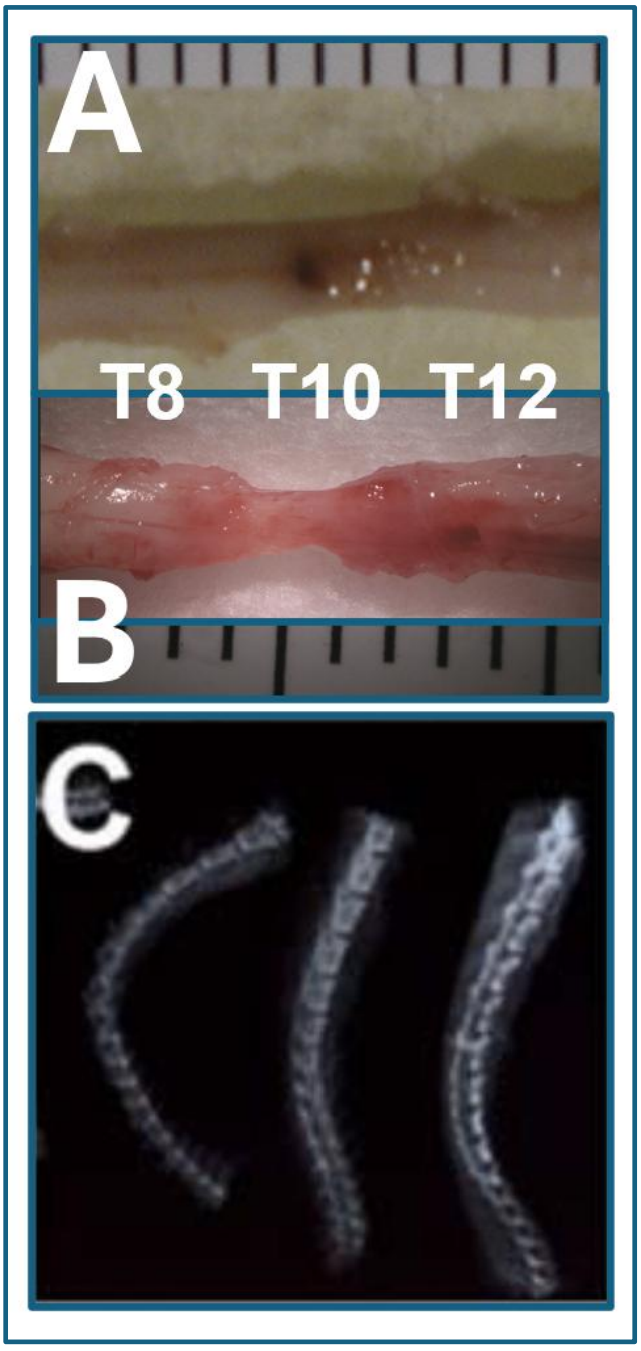

Fig. S1. Structural and radiographic characterization of spinal cord injury after MES. (A) Representative SC at 24 h after paralysis, showing focal hemorrhage and inflammatory changes during the hyperacute phase. **(B)** At 5 days, marked tissue degeneration and loss were evident at the lesion epicenter (T10), with greater involvement at T12 than T8. **(C)** X-ray radiography in 5 stimulated rats showed no vertebral fracture, despite the intense muscle contractions induced by MES, supporting the non-traumatic, ischemic nature of the SCI produced by this protocol.

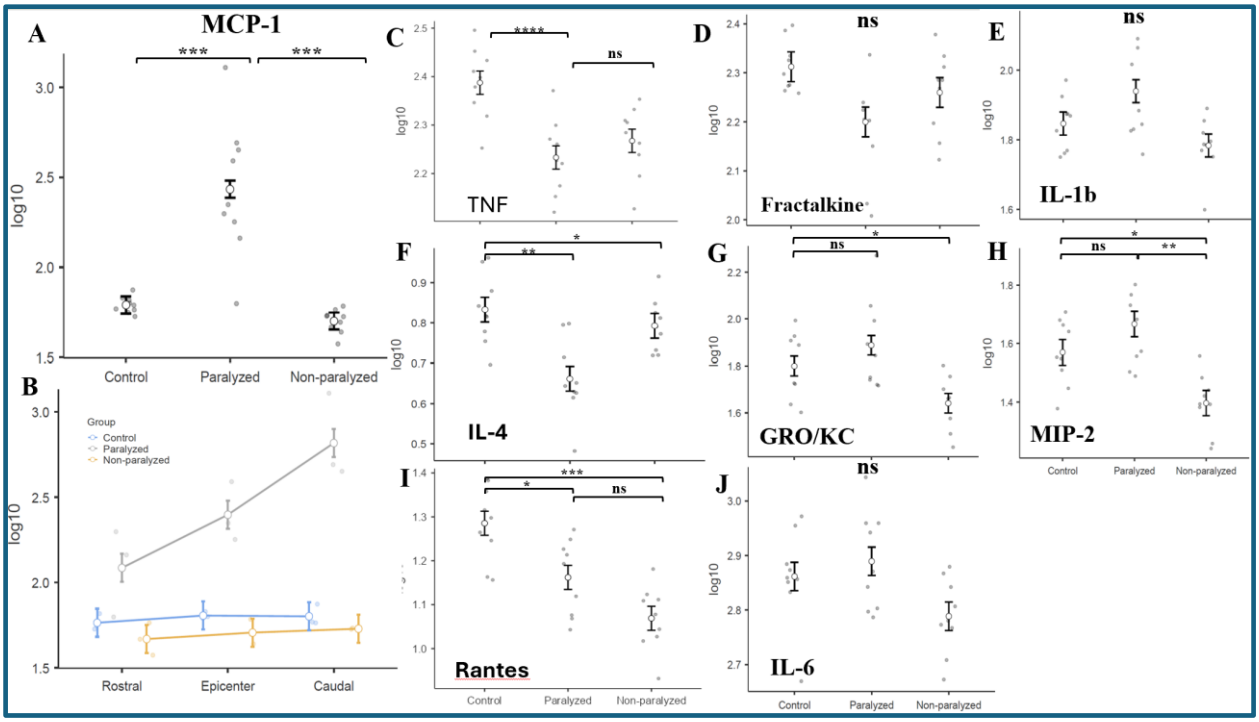

Fig. S2. Regional cytokine and chemokine profiling in acute spinal cord injury. (A–J) Nine cytokines and chemokines previously reported in experimental SCI models and patients were quantified in T8, T10, and T12 SC homogenates 24 h after paralysis using a 9-plex SearchLight® protein array (n = 3 per group). MCP-1/CCL2 showed the most prominent increase, with other mediators displaying regional modulation. The profile supports a temporally and molecularly selective inflammatory response, characterized at 24 h by MCP-1-associated myeloid recruitment and selective suppression/remodeling of cytokine programs, rather than a generalized cytokine surge. Values represent duplicate measurements corrected for sample dilution and expressed as pg/mL. Statistical analysis were performed using ANOVA on Jamovi Software (2.6 version) following concentrations log10 transformation.

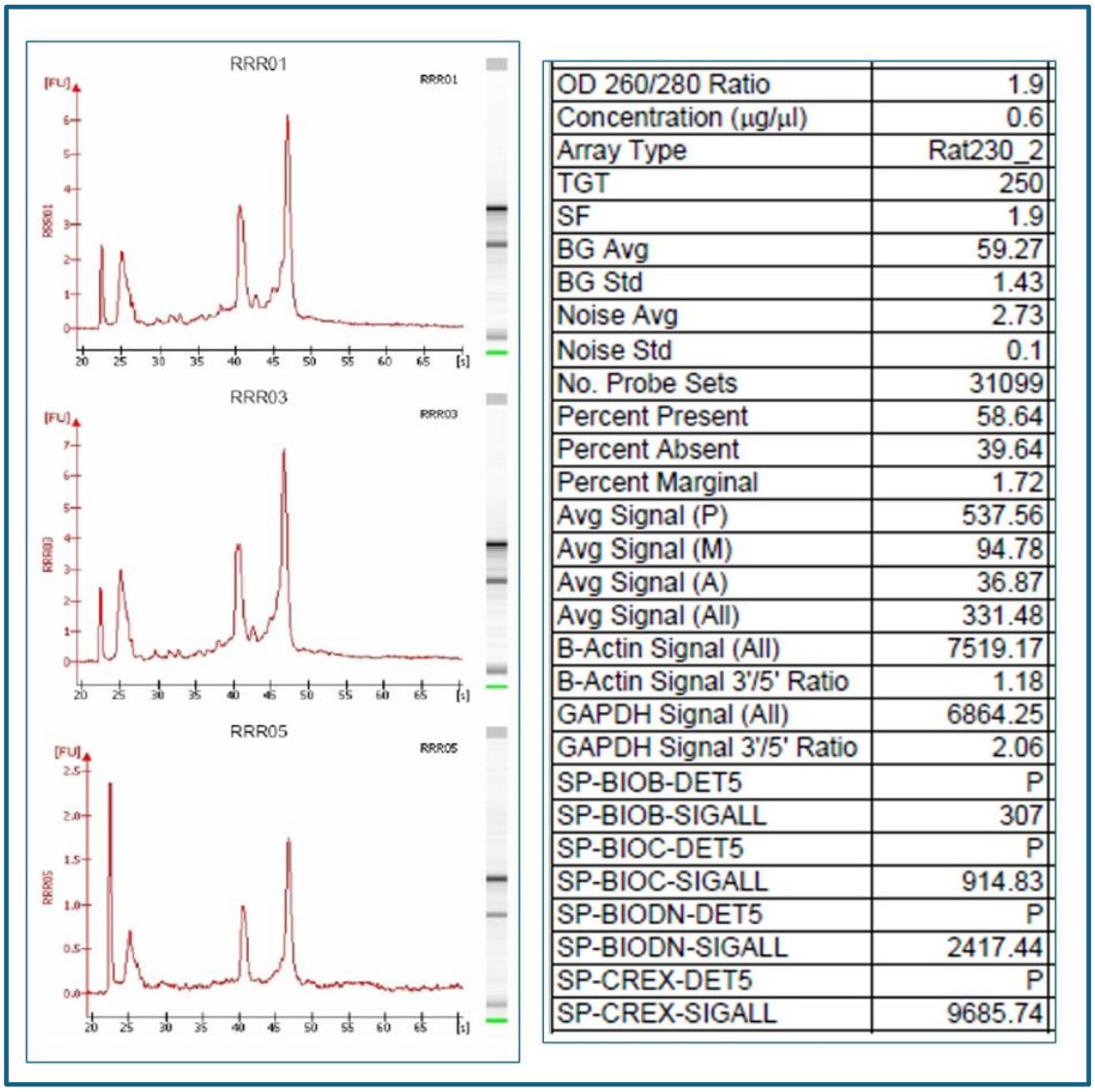

OD 260/280 Ratio	1.9
Concentration (μg/μl)	0.6
Array Type	Rat230_2
TGT	250
SF	1.9
BG Avg	59.27
BG Std	1.43
Noise Avg	2.73
Noise Std	0.1
No. Probe Sets	31099
Percent Present	58.64
Percent Absent	39.64
Percent Marginal	1.72
Avg Signal (P)	537.56
Avg Signal (M)	94.78
Avg Signal (A)	36.87
Avg Signal (All)	331.48
B-Actin Signal (All)	7519.17
B-Actin Signal 3'/5' Ratio	1.18
GAPDH Signal (All)	6864.25
GAPDH Signal 3'/5' Ratio	2.06
SP-BIOB-DET5	P
SP-BIOB-SIGALL	307
SP-BIOC-DET5	P
SP-BIOC-SIGALL	914.83
SP-BIODN-DET5	P
SP-BIODN-SIGALL	2417.44
SP-CREX-DET5	P
SP-CREX-SIGALL	9685.74

Fig. S3. RNA quality assessment of spinal cord samples used for microarray analysis. Representative RNA electropherograms generated by Genome Explorations, Inc. (Memphis, TN, USA) from T10 SC tissue collected 24 h after the onset of paralysis from stimulated paralyzed rats, together with samples collected at the corresponding time point from MES-stimulated non-paralyzed rats and uninjured control animals (bottom to top). All samples displayed the characteristic RNA profile with two prominent ribosomal RNA peaks, with the first peak located at approximately 40 s and the second between 45 and 50 s, consistent with preserved RNA integrity and suitable quality for downstream microarray analysis. The corresponding RNA quality-control summary provided by the analysis software is shown on the right and includes optical density (OD) measurements, RNA concentration, array type, average signal (AVG), and noise for each sample. Samples meeting predefined quality criteria were accepted for downstream transcriptomic analysis.

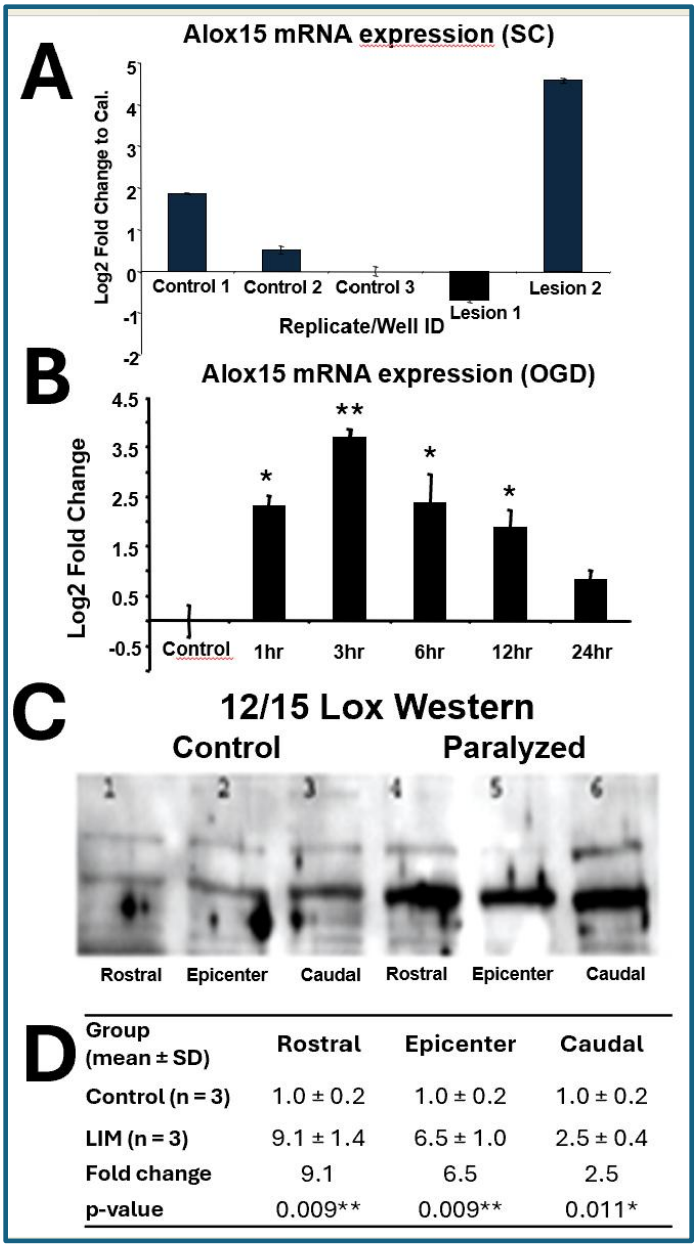

Group (mean ± SD)	Rostral	Epicenter	Caudal
Control (n = 3)	1.0 ± 0.2	1.0 ± 0.2	1.0 ± 0.2
LIM (n = 3)	9.1 ± 1.4	6.5 ± 1.0	2.5 ± 0.4
Fold change	9.1	6.5	2.5
p-value	0.009**	0.009**	0.011*

Fig. S4. Temporal regulation of *Alox15* expression and 12/15-LOX protein after ischemic-like stress and spinal cord injury. (**A**) *Alox15* mRNA expression in spinal cord (SC) tissue at 12 and 24 h after paralysis. A transient approximately fourfold increase was observed at 12 h, followed by reduced expression at 24 h. Data are expressed as log fold change after normalization to *UBC* using the Pfaffl method (2001). (**B**) *Alox15* mRNA expression in primary rat SC astrocytes subjected to oxygen–glucose deprivation (OGD). *Alox15* expression increased transiently during the first 3 h of OGD and subsequently returned toward baseline by 24 h. Data are from three independent experiments, with two technical replicates per condition, normalized to *UBC* and expressed as fold change relative to normoxic controls. $P < 0.05$ versus normoxic controls (one-way ANOVA). (**C**) Representative immunoblot showing 12/15-lipoxygenase (12/15-LOX) protein expression in SC tissue at day 5 after paralysis, with the corresponding loading control. (**D**) Densitometric quantification of 12/15-LOX protein expression in SC tissue at day 5 after paralysis.